Journal of Sound and Vibration (2000) **231**(5), 1396–1412
doi:10.1006/jsvi.1999.3047, available online at http://www.idealibrary.com on IDEAL®

ACTIVE NOISE CONTROL ALGORITHM USING IIR-BASED FILTER

S.-H. Oh and Y. Park

Center for Noise and Vibration Control (NoViC), Department of Mechanical Engineering, Korea Advanced Institute of Science and Technology, Taejon 305-701, *Korea*

(*Received* 5 *December* 1997, *and in final form* 23 *September* 1999)

1. INTRODUCTION

Active noise control algorithms that use the adaptive signal processing technology have been widely investigated and applied in practical situations after Filtered-X LMS algorithm had been proposed by Widrow [1]. The development of Filtered-U LMS algorithm by Eriksson [2] enabled us to control lightly damped systems with long impulse responses or a system with acoustic feedback paths, with a much smaller number of filter weights.

Adaptive FIR or IIR filter structures are usually used for ANC algorithms to reduce undesired noise in time-varying environment. In practical applications, the FIR filter is the most popular because of its stability and linear characteristics. However, adaptive algorithms with FIR structures need a large number of weights to control the lightly damped systems. They try to minimize the error with equal weights for all the frequency components if the reference signal is white noise unless the band pass filters are applied to reference and error signals. In many practical ANC systems, where the reference or desired error signals are narrow band, it is inefficient to control such a system with an FIR filter because we cannot select the control frequency range where the control efforts should be concentrated on.

In this study, a new adaptive filter structure is proposed for ANC systems with banded noise. Constructing an adaptive filter with a linear combination of stable IIR filter bases, we can save much computational power without instability and non-linearity problems, which are usually associated with the conventional IIR adaptive filters. Also, we can selectively choose the control frequencies by appropriately setting the IIR bases. One possible choice for each IIR base is an exponentially enveloped sinusoidal function. The proposed IIR-based adaptive filter needs a smaller number of adaptive weights than the FIR filter for lightly damped systems or narrow banded noise control.

In section 2, an IIR-based filter is proposed and Filtered-X LMS algorithm using the IIR-based filter is derived. Selection of IIR filter bases is discussed in section 3 and three methods to improve the computational efficiency are proposed in section 4. Results of the simulation and the experiment in section 5 demonstrate the feasibility of the proposed algorithm. Conclusions are drawn in section 6.

0022-460X/00/151396 + 17 $35.00/0

2. FILTERED-X LMS ALGORITHM USING IIR-BASED FILTER

2.1. IIR BASED FILTER

When an FIR structure is used for ANC, a sufficiently large number of filter weights are necessary to maintain desired control performance especially for a lightly damped system. The necessary computational power can be reduced using an IIR structure with a smaller number of weights; however this may cause instability and non-linearity problems in the adaptive update process of filter weights. To eliminate these problems, an IIR-based filter, which is a linear combination of fixed stable IIR filters, is proposed as follows:

$$B(q^{-1}) = \sum_{i=1}^{L} w_i B_i(q^{-1}). \tag{1}$$

where

$$B_i(q^{-1}) = \frac{C_i(q^{-1})}{1 - A_i(q^{-1})}. \tag{2}$$

$$A_i(q^{-1}) = a_{i1}q^{-1} + a_{i2}q^{-2} + \cdots, C_i(q^{-1}) = c_{i0} + c_{i1}q^{-1} + c_{i2}q^{-2} + \cdots. \tag{3}$$

w_i is a weight of the ith IIR filter base $B_i(q^{-1})$ and $B_i(q^{-1})$ must be predetermined appropriately by the designer. The determination procedure is discussed in section 3.

Filter output $y(k)$ at a discrete time instant k is given by

$$y(k) = B(q^{-1})x(k) = \sum_{i=1}^{L} w_i B_i(q^{-1})x(k) = \sum_{i=1}^{L} w_i u_i(k), \tag{4}$$

where $u_i(k)$ is an output of the IIR filter with the input of $x(k)$. Hence IIR-based filter output, $y(k)$, is expressed as a linear combination of $u_i(k)$, $i = 1, \ldots, L$. The proposed IIR-based filter has an infinite impulse response, but it does not have any non-linearity or instability problems in updating filter weights contrary to the conventional IIR filter.

If $A_i(q^{-1}) = 0$ and $B_i(q^{-1}) = q^{-i+1}$ in equation (1), the proposed IIR-based filter becomes identical to a conventional FIR filter with length L. Therefore, the FIR structure can be considered as a subset of the IIR-based filter structure.

2.2. FILTERED-X LMS ALGORITHM FOR IIR BASED FILTER STRUCTURE

Assume that the error path H is represented by a FIR filter of order $M + 1$, $H = [h_0, h_1, \ldots, h_M]^{\mathrm{T}}$, $d(k)$ is the desired signal, and $u_i(k)$ is the filtered signal of the reference $x(k)$ through the ith IIR filter base. The residual error $e(k)$, which is detected by the error microphone, is expressed as

$$e(k) = d(k) - \sum_{i=0}^{M} h_i \mathbf{w}(k-i)^{\mathrm{T}}\mathbf{u}(k-i). \tag{5}$$

where

$$\mathbf{w}(k) = [w_1(k), w_2(k), \ldots, w_L(k)]^{\mathrm{T}}, \quad \mathbf{u}(k) = [u_1(k), k_2(k), \ldots, u_L(k)]^{\mathrm{T}}. \tag{6}$$

The jth weight of the IIR-based filter is updated by $U_j(k)$, whose elements are subsequently filtered signal through the jth base filter as follows:

$$w_j(k+1) = w_j(k) + 2\mu e(k)\hat{H}^{\mathrm{T}}U_j(k), \tag{7}$$

$$U_j(k) = [u_j(k), u_j(k-1), \ldots, u_j(k-M)]^{\mathrm{T}}, \tag{8}$$

where $\hat{H}$ is the estimated model of the error path. In vector form, equation (7) can be rewritten as

$$\mathbf{w}(k+1) = \mathbf{w}(k) + 2\mu e(k)\mathbf{U}^{\mathrm{T}}\hat{H}, \tag{9}$$

where

$$\mathbf{U} = [U_1(k), U_2(k), \ldots, U_L(k)] = \begin{bmatrix} u_1(k) & u_2(k) & \cdots & u_L(k) \\ u_1(k-1) & u_2(k-1) & \cdots & u_L(k-1) \\ \vdots & \vdots & \vdots & \vdots \\ u_1(k-M) & u_2(k-M) & \cdots & u_L(k-M) \end{bmatrix} = \begin{bmatrix} \mathbf{u}(k)^{\mathrm{T}} \\ \mathbf{u}(k-1)^{\mathrm{T}} \\ \vdots \\ \mathbf{u}(k-M)^{\mathrm{T}} \end{bmatrix}. \tag{10}$$

Figure 1 shows the block diagram of the Filtered-X LMS algorithm using the IIR-based filter structure. Stability analysis is almost the same as in previous work done by Kim [3], and therefore, is omitted in this paper.

If we increase the number of IIR filter bases, a larger amount of reduction can be achieved because the controlled frequency region is extended. But because the necessary computation power increases as well, the number of IIR bases should be properly chosen.

If the reference signal is composed of n number of frequency components, perfect attenuation of the residual error is possible with $2n$ or more IIR filter bases. It is the same with the underdetermined case of the conventional algorithm with FIR filter. In general, however, perfect cancellation is not possible for overdetermined cases in which half the number of IIR filter bases is less than the number of frequency components of the reference signal, except where the gain of the proposed adaptive filter exactly becomes $H^{-1}(\mathrm{j}\omega)P(\mathrm{j}\omega)$ in all of the control frequency range.

3. DETERMINATION OF IIR FILTER BASE

Better choice of IIR filter base can effectively enhance the performance, convergence speed and calculation efficiency. In this paper, we adopt an exponentially enveloped sinusoidal function as an impulse response of each IIR filter base among several candidates, such as modified Legendre functions [4], Bessel functions and the other orthogonal functions [5]. Sinusoidal functions are orthogonal to each other, but exponential sinusoidal functions are orthogonal only approximately. Its orthogonality depends on the decaying envelope of the exponential function. There are two parameters to be determined for each base function. One is the fundamental sinusoidal frequency, which determines the

control frequency range and the other is the time constant of the exponential function, which controls the orthogonality.

Consequently, an IIR-based filter becomes a Prony model [6], which represents a time series as the sum of complex exponential functions. Each IIR base is described in the z-domain as follows:

$$B_{i,c}(z) = \frac{1 - e^{-\sigma_i T} z^{-1} \cos \omega_i T}{1 - 2e^{-\sigma_i T} z^{-1} \cos \omega_i T + e^{-2\sigma_i T} z^{-2}},$$

$$B_{i,s}(z) = \frac{e^{-\sigma_i T} z^{-1} \sin \omega_i T}{1 - 2e^{-\sigma_i T} z^{-1} \cos \omega_i T + e^{-2\sigma_i T} z^{-2}}, \quad i = 1, \ldots, L. \tag{11}$$

$B_{i,c}(z)$ and $B_{i,s}(z)$ are z transforms of $e^{-\sigma_i t} \cos \omega_i t$ and $e^{-\sigma_i t} \sin \omega_i t$, respectively. Two IIR bases, $B_{i,c}(z)$ and $B_{i,s}(z)$ with real coefficients, are needed to describe the magnitude and phase of a system at frequency ω_i. Appropriate ω_i and σ_i in equation (11) can be easily determined by the Prony method [6, 7] as long as the nominal desired model to be approximated is known. A determination procedure by the Prony method is detailed in Appendix A.

There exists the optimal set of ω_i, σ_i and weights of IIR bases to attenuate undesired noise. However, it is not easy to get the optimal set with adaptive determination of all the values at the same time because an IIR-based adaptive filter with respect to these values are non-linear. Hence, we separated the parameter selection procedure into two parts. The number of IIR base, center frequencies and the damping ratios are pre-determined before control and has fixed values on control process, and only the weights of IIR bases are estimated during the adaptation process. We cannot say that the parameters of the IIR-based adaptive filter converges to one of the optimal set via the proposed off-line algorithm. There may be an algorithm for finding an optimal set of parameters, but the algorithm may have more complicated structure and require high computational power than the proposed algorithm. In practical applications, it would be better to use a simple and efficient algorithm with a little performance degradation.

4. REDUCTION METHOD OF NECESSARY COMPUTATIONAL LOAD

4.1. THE METHOD BASED ON LINEAR RELATION BETWEEN THE ERROR PATH AND BASE FILTERS

In Filtered-X LMS algorithm based on IIR-based filter structure in Figure 1, each $u_i(k)$ must be filtered through the error path model in order to update $w_i(k)$. Consequently, the number of filterings through the error path model increases to L times of the conventional Filtered-X LMS algorithm and the required computational power increases considerably.

One method of reducing the computational load is to exchange the sequence of the error path model and base filters as shown in Figure 2. The number of filterings through B_i increases to twice those of the original algorithm, but the error path filtering is reduced to just one. Hence, this method saves much computation especially for the cases when the error path has a long impulse response. There is no

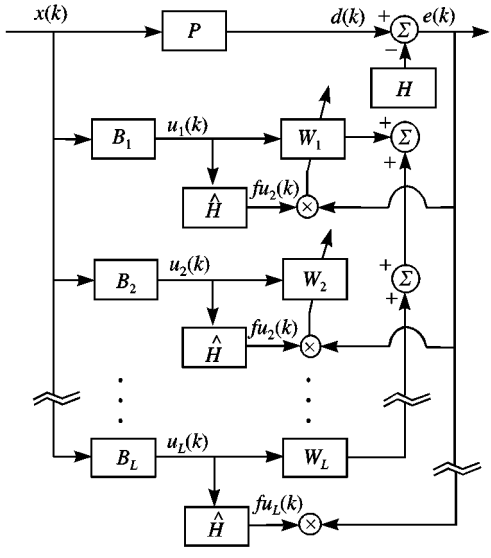

Figure 1. Filtered-X LMS algorithm using IIR-based filter.

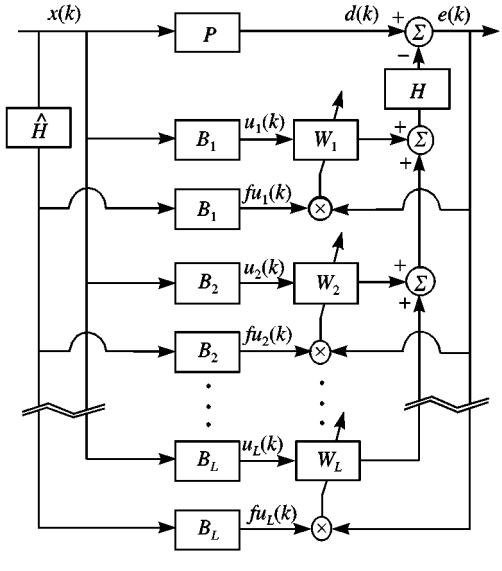

Figure 2. First method reducing computational road; exchanging H and B_i.

performance degradation because of the equivalence between the modified and the original algorithm.

4.2. INTRODUCTION OF DELAYED INVERSE ERROR PATH MODEL

We can reduce the computational load by modifying the original algorithm based on a delayed inverse model [1, 2] of the error path. The block diagram is

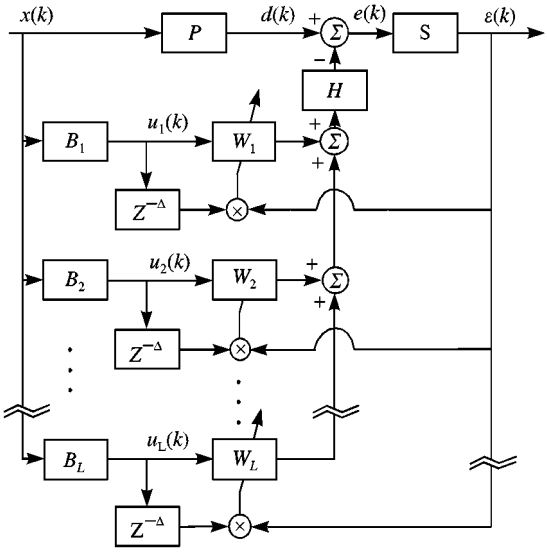

Figure 3. Second method reducing computational road; delayed inverse error path model are used instead of it.

shown in Figure 3. The delayed inverse model S, where $S = [s_0, s_1, \ldots, s_N]^{\mathrm{T}}$, satisfies the equation

$$\sum_{j=0}^{N} \sum_{i=0}^{M} s_j h_i x(k - i - j) = x(k - \Delta), \tag{12}$$

and the weighted error $\varepsilon(k)$ can be defined as follows:

$$\varepsilon(k) = \sum_{j=0}^{N} s_i \mathrm{e}(k-1) = \sum_{j=0}^{N} s_j d(k-j) - \mathbf{w}(k-\Delta)^{\mathrm{T}} \mathbf{u}(k-\Delta), \tag{13}$$

where Δ is a design parameter which enables us to evaluate the delayed inverse model considering the causality of the error path. The weight update equation which minimizes the weighted mean-square error $\varepsilon^2(k)$ is given by

$$\mathbf{w}(k+1) = \mathbf{w}(k) + 2\mu\varepsilon(k)\mathbf{u}(k-\Delta). \tag{14}$$

The heavy computational burden in the original algorithm is reduced because the error path model filtering is not needed in updating the weights in equation (14). It needs just one filtering through the delayed inverse model to make the weighted error instead of L time filtering through the error path model in the original algorithm.

Stable μ bound of the algorithm using the delayed inverse model in the mean sense can be easily derived as follows:

$$0 < \mu < \sin\left\{\frac{\pi}{2(2\Delta+1)}\right\} \Big/ \lambda_{max}, \tag{15}$$

where λ_{max} is the largest eigenvalue of the correlation matrix of $\mathbf{u}(k)$.

As Δ gets smaller in equation (15), the stable μ bound of the algorithm becomes bigger. The causality constraint should be satisfied in designing the delayed inverse model, i.e., Δ must be larger than the group delay of the real error path. As a rule of thumb, we let Δ be half the length of the delayed inverse model [1]. It is desirable to let Δ be as small as possible for fast convergence speed. Thus, Δ should be designed carefully considering the causality and the convergence speed.

It is noted that the weighted mean-square error $\varepsilon^2(k)$ is minimized instead of $e^2(k)$ in this reduction method, and so there may be a little performance degradation.

4.3. SIMPLIFICATION OF ERROR PATH MODEL

When the impulse response of each base filter is designed as an exponential sinusoidal function, it is possible to simplify the error path model with two constants. It saves much computation for the error path that has a long impulse response.

The signal filtered with the base filter must be re-filtered through the error path model to update the weights. For small σ_i, the output, filtered through the ith IIR base, $B_{i,c}(j\omega)$ or $B_{i,s}(j\omega)$, get close to a tonal signal with frequency ω_i. We can model the error path only with the magnitude and phase information at $\omega = \omega_i$. As shown in Figure 4, the signal filtered through the error path model can be approximated as a linear combination of $u_{i,c}(k)$ and $u_{i,s}(k)$ by choosing $\alpha_{i,c}$, $\alpha_{i,s}$, $\beta_{i,c}$ and $\beta_{i,s}$ properly. We can derive the following approximations to get $\alpha_{i,c}$, $\alpha_{i,s}$, $\beta_{i,c}$ and $\beta_{i,s}$ from Figure 4:

$$\begin{aligned} B_{i,c}(j\omega_i)\hat{H}(j\omega_i) &\approx \alpha_{i,c}B_{i,c}(j\omega_i) + \alpha_{i,s}B_{i,s}(j\omega_i), \\ B_{i,s}(j\omega_i)\hat{H}(j\omega_i) &\approx \beta_{i,c}B_{i,c}(j\omega_i) + \beta_{i,s}B_{i,s}(j\omega_i), \end{aligned} \tag{16}$$

where $\alpha_{i,c}$, $\alpha_{i,s}$, $\beta_{i,c}$ and $\beta_{i,s}$ are constant coefficients multiplied to base filters instead of the error path model.

On the other hand, Fourier transforms of $B_{i,c}(j\omega)$ and $B_{i,s}(j\omega)$ of equation (11) are expressed as

$$\begin{aligned} B_{ic}(j\omega) &= \frac{1}{2}\left(\frac{1}{-\sigma_i + j(\omega - \omega_i)} + \frac{1}{-\sigma_i + j(\omega + \omega_i)}\right), \\ B_{is}(j\omega) &= \frac{1}{2}\left(\frac{1}{-\sigma_i + j(\omega - \omega_i)} + \frac{1}{-\sigma_i + j(\omega + \omega_i)}\right), \end{aligned} \tag{17}$$

Substituting equation (17) into equation (16) and after some algebraic manipulations, $\alpha_{i,c}$, $\alpha_{i,s}$, $\beta_{i,c}$ and $\beta_{i,s}$ are obtained as

$$\begin{Bmatrix} \alpha_{ic} \\ \alpha_{is} \end{Bmatrix} = \begin{bmatrix} 1 & \dfrac{-\sigma_i}{\omega_i} \\ 0 & \dfrac{a_i^2 + \omega_i^2}{\omega_i^2} \end{bmatrix} \begin{Bmatrix} \mathrm{Re}[H(j\omega)] \\ \mathrm{Im}[H(j\omega)] \end{Bmatrix}. \tag{18}$$

$$\begin{Bmatrix} \beta_{ic} \\ \beta_{is} \end{Bmatrix} = \begin{bmatrix} 0 & 1 \\ 1 & \dfrac{\omega_i}{\sigma_i} \end{bmatrix} \begin{Bmatrix} \mathrm{Re}[H(j\omega)] \\ \mathrm{Im}[H(j\omega)] \end{Bmatrix}. \tag{19}$$

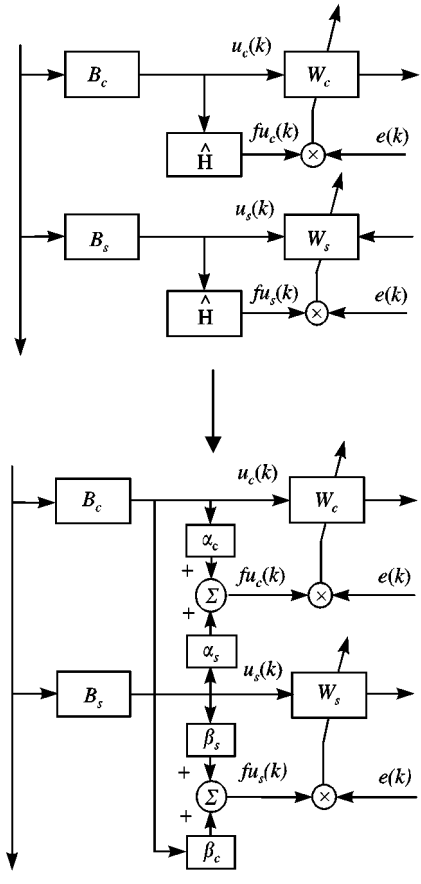

Figure 4. Third method reducing computational road; simplification of error path model.

The weight update equation for the modified algorithm is given as follows:

$$\mathbf{w}(k+1) = \mathbf{w}(k) + 2\mu e(k)\mathbf{C}\mathbf{u}(k), \tag{20}$$

where

$$\mathbf{C} = \begin{bmatrix} \alpha_{1c} & \alpha_{1s} & & & \mathbf{0} & \mathbf{0} \\ \beta_{1c} & \beta_{1s} & & & & \\ & \mathbf{0} & & \ddots & & \mathbf{0} \\ & & & & \alpha_{Lc} & \alpha_{Ls} \\ & \mathbf{0} & & \mathbf{0} & & \\ & & & & \beta_{Lc} & \beta_{Ls} \end{bmatrix}, \tag{21}$$

$$\mathbf{w}(k) = [w_{1c}(k), w_{1s}(k), \ldots, \mathbf{w}_{1c}(k), w_{1s}(k)]^{\mathrm{T}}, \tag{22}$$

$$\mathbf{u}(k) = [u_{1c}(k), u_{1s}(k), \ldots, u_{Lc}(k), u_{Ls}(k)]^{\mathrm{T}}. \tag{23}$$

If the error path is an n step pure delay system with unit magnitude, the stable μ bound satisfies the following inequality:

$$0 < \mu < \sin\left\{\frac{\sin(\phi/2)}{\lambda_i[\mathbf{CR}_{uu}(-n)]}\right\}_{min}, \qquad \phi_i = \frac{\pi + 2\angle\lambda_i[\mathbf{CR}_{uu}(-n)]}{2n+1}, \tag{24}$$

where $\mathbf{R}_{uu}$ is the correlation matrix of $\mathbf{u}(k)$ and $\lambda[\cdot]$ means the ith eigenvalue of a given matrix. Bode plots of the simplified error path model and the original error path are drawn in Figure 5. Because the two systems are different at all frequencies except ω_i, the signal filtered through the simplified error path model is also different from the signal filtered through the error path and it may degrade the control performance. If the phase difference at the neighbourhood frequency component of ω_i, which is dominant in filtered signal, is greater than 90°, the IIR-based filter weights of the algorithm using the simplified error path model would diverge.

In general, the larger the group delay of the error path is, the larger the phase difference between the two systems is. Because of this, it is difficult to simplify the error path model for a system which has a large group delay.

Table 1 shows the comparison of the computational loads among the Filtered-X LMS algorithm using the IIR-based filter, three proposed methods for reducing the computational load and the conventional Filtered X-LMS algorithm.

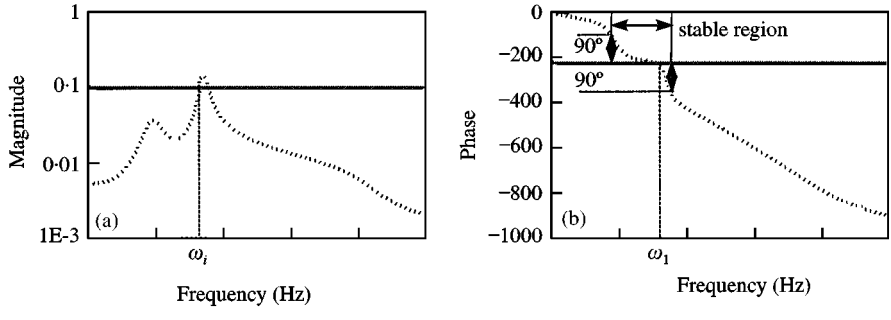

Figure 5. Bode plots of error path and simplified error path model. ..... error path; —— simplified error path model. (a) Magnitude plot. (b) Phase plot.

TABLE 1

Comparison of computational power for FIR filter and discrete IIR-based filter (L *is the length of FIR filter for Filter-X LMS algorithm and the number of IIR bases for the proposed algorithm,* M *is the length of the error path model*)

	FIR filter	IIR-based filter			
Computations	Filtered-X LMS algorithm	Filtered-X LMS algorithm	Filtered-X LMS algorithm + method I	Filtered-X LMS algorithm + method II	Filtered-X LMS algorithm + method III
×	$2L+M+1$	$5L+ML+1$	$8L+M+1$	$5L+M+1$	$7L+1$
+	$2L+M-2$	$4L+ML-1$	$8L+M-2$	$5L+M-2$	$6L-1$

TABLE 2

Comparison of computational power for FIR filter and analog IIR-based filter (L is the length of FIR filter for Filter-X LMS algorithm and the number of IIR bases for the proposed algorithm, M is the length of the error path model)

	FIR filter	IIR-based filter			
Computat-ions	Filtered-X LMS algorithm	Filtered-X LMS algorithm	Filtered-X LMS algorithm + method I	Filtered-X LMS algorithm + method II	Filtered-X LMS algorithm + method III
×	$2L + M + 1$	$2L + ML + 1$	$2L + M + 1$	$2L + M + 1$	$4L + 1$
+	$2L + M - 2$	$L + ML - 1$	$2L + M - 2$	$2L + M - 2$	$3L - 1$

L is the number of base filters and the FIR filter length and M is the error path length. Method 1 is the reduction method based on the linear relationship between the error path and the IIR bases. Method II is the reduction method based on the delayed inverse model and method III represents the reduction method using the simplified error path model.

Method I and II need at most 4 times and 2·5 times more computational power than the conventional algorithm respectively. Method III may use less computation than the conventional algorithm. If the acoustic plant and the error path are lightly damped systems in which we expect that the proposed IIR-based filter is more efficient than the conventional FIR adaptive filter, the computational load of method III is much smaller than that of others.

In order to reduce the necessary computation power, an IIR filter of analog structure can also be used as a base filter. The computational powers for analog bases are listed in Table 2. Because any further computation is not needed for filtering through the analog IIR base, methods I and II require the same amount of computation with the conventional algorithm.

5. SIMULATION AND EXPERIMENTAL RESULTS

5.1. SIMULATION RESULTS

Performances and transient responses for the IIR-based filter are compared with those of the algorithm using FIR filter through the simulation.

Figure 6 shows the impulse responses of the plant and the error path used in the simulation and pole/zero map of the plant. There are two lightly damped poles in the plant. Center frequencies and damping coefficients were determined by the Prony method [7] as follows:

$$\begin{aligned} \omega_1 &= 2\pi \times 195 \text{ rad/s}, \quad \sigma_1 = 164, \\ \omega_2 &= 2\pi \times 342 \text{ rad/s}, \quad \sigma_1 = 70. \end{aligned} \tag{25}$$

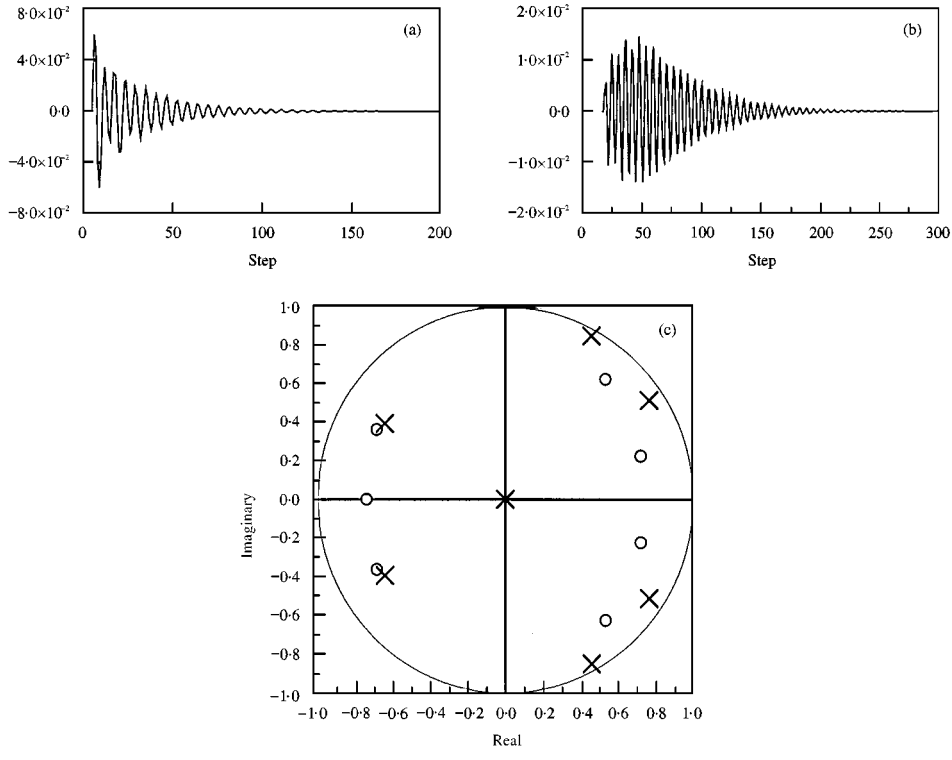

Figure 6. Impulse responses of the simulation system. (a) Impulse response of the error path. (b) Impulse response of the plant. (c) Pole zero map of the plant

If the nominal plant is unknown, the parameters of the base filters must be selected by trial and error. If the combination of the four IIR bases designed with the parameters of equation (25) are used in the IIR-based filter, just two frequency components of the undesired noise are attenuated. Hence nine center frequencies, $\omega_i = 175, 195, 215, 322, 332, 342, 352, 362, 380$ Hz were selected and damping coefficients were reduced to 100 for the first three frequencies and 50 for the others in order to extend the control frequency range. All of the IIR bases were discrete filter expressed in equation (11). The conventional Filtered-X LMS algorithm with 72 weights was also used to control the same plant. Two algorithms require almost the same computational power. The reference signal was Gaussian white noise and the error path was modelled as a FIR filter with 100 taps. Three reduction method of computation power are used in the simulation. Figure 7 shows the time responses before and after control. Convergence speed and steady state responses with the FIR filter are similar to those with 18 IIR filter bases. Error spectra at steady state before and after ANC are shown in Figure 8. The IIR-based filter has a better steady state response than the FIR filter in 320–380 Hz. The degradation of the performance appeared when the delayed inverse model is used.

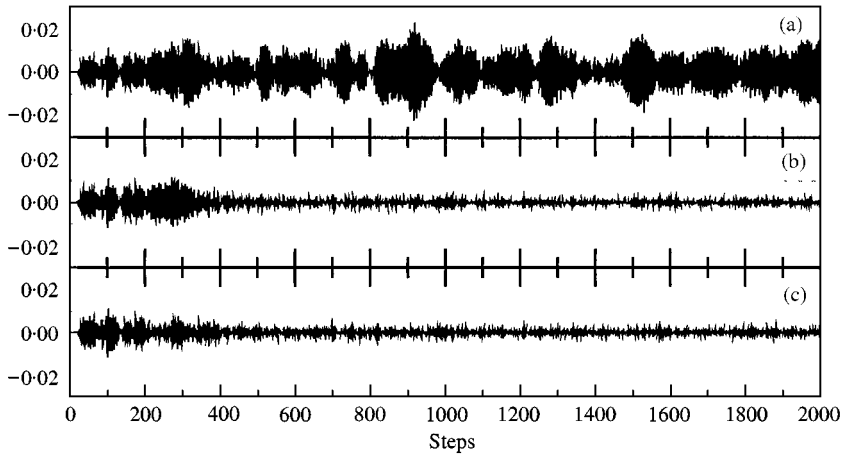

Figure 7. Time responses of the error signal before and after ANC in simulation: (a) Before ANC, (b) after ANC with FIR filter (72 weights), (c) after ANC with IIR-based filter (18 weights).

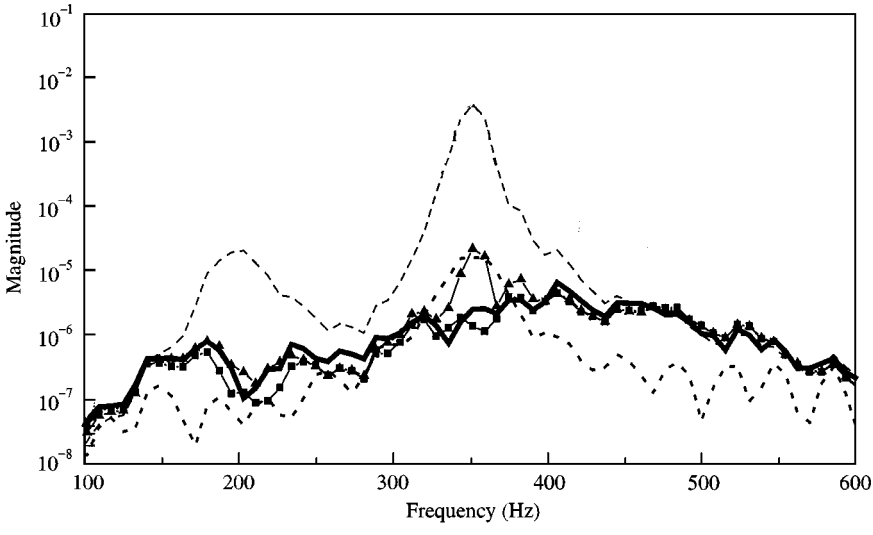

Figure 8. Error spectra before and after ANC in simulation; – – – – before ANC, —— after ANC with IIR-based filter (18 weights), ... after ANC with FIR filter (72 weights), –△– after ANC with delayed inverse filter, –□– after ANC with simplified error path model.

5.2. EXPERIMENTAL RESULTS

The figure of the three-dimensional half-scale car cabin used in the experiment and the frequency response function of its model are shown in Figure 9. We easily find that there are several resonant peaks in the cabin model. The primary source was located in front of the driver seat. In order to reduce the noise near the driver's head, the error microphone was located at the front left roof of the cabin and the secondary source was located at the center of the roof.

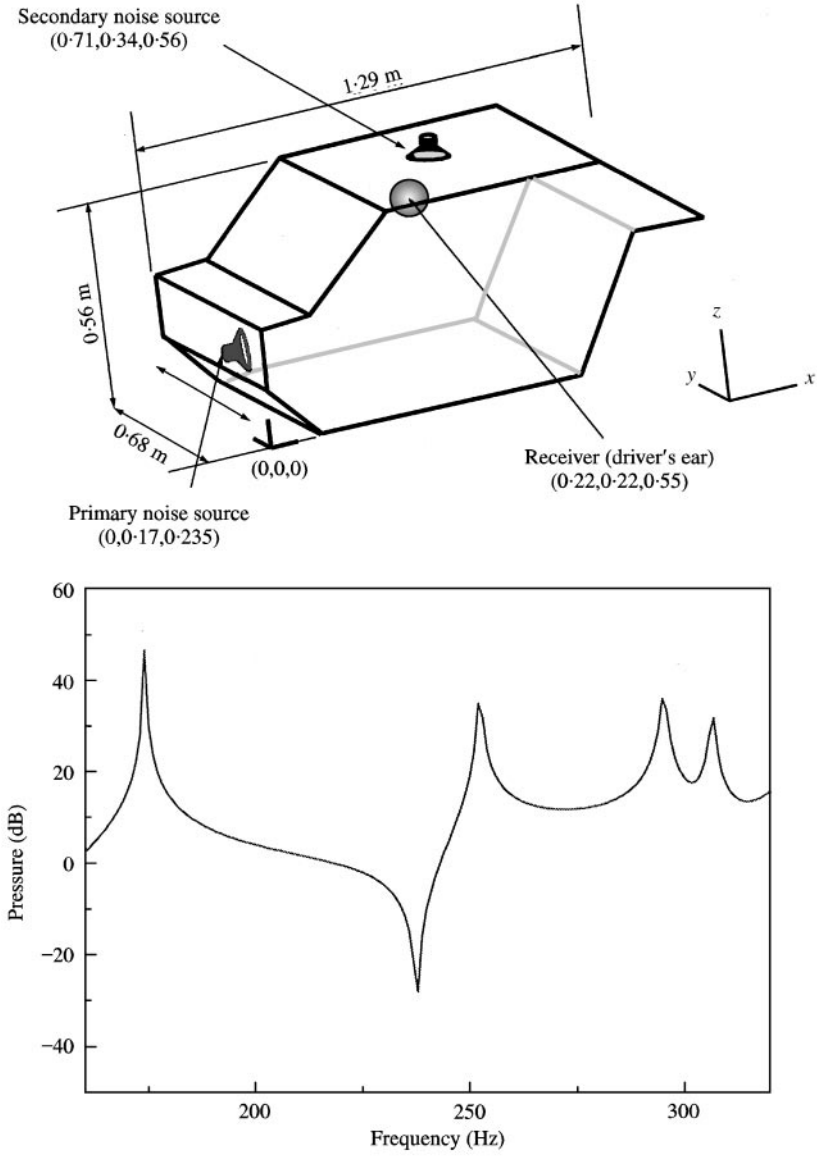

Figure 9. Half-scale car cabin model for ANC experiments. (a) Half-scale car cabin. (b) FRF of the half-scale car cabin model.

Hundred hertz banded noise centered at 250 Hz was used for both the reference signal and the primary source input in order to observe the control performance near the natural frequencies of the cabin (174, 260, 280, 307 and 345 Hz). Six base filters with $\omega_i = 257, 260, 263$ Hz and $\sigma_i = 20$ are selected to control the noise near 260 Hz. The other 12 filter bases which have center frequencies at 275, 280, 285, 305, 310, 315 Hz with $\sigma_i = 40$ were added to reduce the undesired noise near 280 and 307 Hz. Eighteen IIR filters of the second order were used as an IIR-based filter and

the first method of reducing computational load was used in this experiment. To compare the control performance, the FIR filter of 256 taps was used for the adaptive filter. The error path was modelled as a FIR filter of 256 length for both cases. For the experiment, a TMS320c40 DSP chip, board and a 20 input 8 output AD/DA converter in connection with a notebook computer were used with a 2 kHz sampling rate.

Figure 10 shows the experimental results for two adaptive filters. Two control performances using an 256 FIR filter and an 18 IIR-based filter are similar in the selected frequency ranges even though the computational power of the proposed algorithm is one-third of that of the algorithm using the 256 FIR filter. When we used an 128 FIR filter, the residual error around 260 Hz was not attenuated sufficiently. Note that there is little reduction of noise in controlled spectrum using an IIR-based filter around 175 and 345 Hz where we have some amount of reduction with an FIR filter, because no IIR filter base is located in these frequencies ranges. The characteristics of IIR-based algorithm can be useful for reducing the noise selectively.

In this experiment, one error microphone and one control speaker were used and so we can get an improved control performance with the FIR filter by increasing the filter length. However, it is not easy to increase the filter length for a multi-channel system in which the computational power is limited. For this case, the IIR-based filter can achieve better control performance than the FIR filter.

Simulation and experimental results demonstrate that the proposed adaptive filter may provide an efficient alternative to the conventional FIR filter for ANC/AVC applications that require much computation and a selective frequency range of reduction. There are, however, some drawbacks: design parameters, such

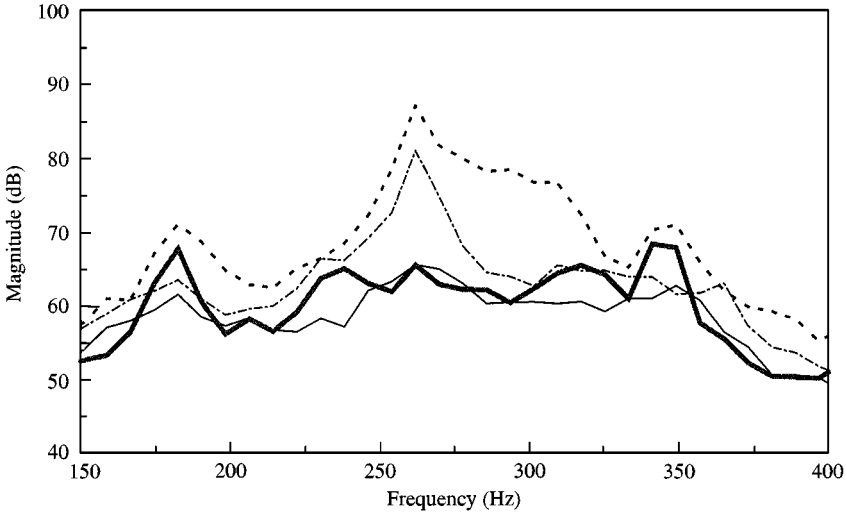

Figure 10. Error spectra before and after ANC in experiment; ---- before ANC ▬▬ after ANC with IIR-based filter (18 weights), —— after ANC with FIR filter (256 weights), –·–·–·– after ANC with FIR filter (128 weights).

as center frequencies and damping coefficients of the IR filter bases, need to be determined before control with some plant information to get better performance.

Among the three proposed methods of reducing the computational load, method I has better performance than others although it does require more computation. Method III has the demerit that it can be used only when the error path has a small delay even though it requires less computational power than the others. The delayed inverse error path model can be applied to systems with relatively large group delay: however, there is a little performance degradation.

The proposed method is a viable alternative to the conventional FIR filter-based algorithm especially when the selected frequency ranges of the noise to be reduced or the dominant noise frequencies are known *a priori*.

6. CONCLUSIONS

We have described a new adaptive filter, the so-called IIR-based filter, which consists of fixed stable IIR filters. We can control undesired noise for a lightly damped system with a smaller number of filter weights and less computational power than those of the FIR filter. The proposed adaptive filter has an IIR structure but does not have instability and non-linearity problems commonly associated with the conventional IIR filter structure. It is possible to control only the desired frequency range by choosing proper IIR-based filters.

To prevent the increase of the required computational power with an IIR-based filter, three methods to reduce the computational load were also proposed. By exchanging the filtering order between base filters and the error path model, we can reduce the computational power without performance degradation. The delayed inverse model of the error path can also be used to reduce the computational power. There may be, however, a little performance degradation. When the group delay of the error path is small, we can simplify the error path model as two constant coefficients. Feasibility of the proposed scheme is demonstrated through the simulation and the experiment.

REFERENCES

1. WIDROW 1985 *Adaptive Signal Processing*. Englewood Cliffs NJ: Prentice-Hall.
2. L. J. ERIKSSON 1991 *Journal of the Acoustical Society of America* **89**, 257–265. Development of the Filtered-U algorithm for active noise control.
3. HYOUN-SUK KIM 1993 *M.S. Thesis KAIST* 12-23. ANC algorithm for a duct system with reduced computational burden and fast convergence.
4. HECTOR PERES AND SHIGEO TSUJII 1991 *IEEE Transactions on Signal Processing* **39**, 752–755. A system identification algorithm using orthogonal functions.
5. JAMES THI AND ALCLAUS 1993 *Proceedings of the Recent Adavances in Active Control of Sound and Vibration. VI, U.S.A.* **1**, 535–542. A new adaptive filter with orthogonal second order sections for active noise control.
6. F. B. HILDEBRAND 1956 *Introduction to Numerical Analysis*. New York: McGraw-Hill.
7. P. DAVIES 1983 *Journal of Sound and Vibration* **89**, 571–583. A recursive approach to prony parameter estimation.

8. S. D. SNYDER AND C. H. HANSEN 1990 *Journal of Sound and Vibration* **141**, 409–424. The influence of tranducer transfer-functions and acoustic time delays on the implementation of the LMS algorithm in active noise control systems.

APPENDIX A

The modelling of a system with an adaptive filter composed of IIR bases can be thought of as one of the curve-fitting methods. When the bases are expressed as exponential sinusoidal functions, it is the same with the Prony series method, which is to fit a series of complex exponentials to a time series. This method can be used to find the natural frequencies, damping coefficients and amplitudes easily. An impulse response of a system can be expressed as follows:

$$y(k) = \sum_{i=1}^{N} A_i x_i^k + e(k), \tag{A1}$$

where

$$x_i = \mathrm{e}^{(\sigma_i + \mathrm{j}\omega_i)T}, \quad i = 1, 2, \ldots, N. \tag{A2}$$

A_i is a scalar coefficient, σ_i and ω_i are the damping coefficient and the radial frequency respectively, T is the sampling time and $e(k)$ is the residual error. Our goal is to find x_i, $i = 1, 2, \ldots, N$. Suppose the following complex polynomial whose roots are x_is:

$$\sum_{k=0}^{N} a_k x^k = \prod_{i=1}^{N} (x - x_i). \tag{A3}$$

if we replace x^k of equation (3) with $y(\mathrm{j} + k)$ then the following equation holds:

$$\begin{aligned} \sum_{k=0}^{N} a_k y(\mathrm{j} + k) &= \sum_{k=0}^{N} a_k \left(\sum_{i=1}^{N} A_i x_i^{j+k} + e(\mathrm{j} + k) \right) \\ &= \sum_{i=0}^{N} A_i x_i^j \left(\sum_{k=1}^{N} a_k x_i^k \right) + \sum_{k=0}^{N} a_k e(\mathrm{j} + k). \end{aligned} \tag{A4}$$

The first term on the right-hand side of equation (A4) is zero, for x_i is a root of equation (A3). If the residual error $e(\mathrm{j} + k)$ is much smaller than unity, the second term can also be neglected. Therefore, we can rewrite equation (A4) as

$$\sum_{k=0}^{N} a_k y(\mathrm{j} + k) \cong 0. \tag{A5}$$

From equation (A5), we can easily find the least-squares solution of $\mathbf{Qa} = \mathbf{b}$ which minimizes the term $\sum_{k=0}^{N} a_k e(\mathrm{j} + k)$ in a least-squares sense as follows:

$$\mathbf{a} = [\mathbf{Q}^{\mathrm{T}}\mathbf{Q}]^{-1}\mathbf{Q}^{\mathrm{T}}\mathbf{b}, \tag{A6}$$

where

$$\mathbf{Q} = \begin{bmatrix} y(0) & \cdots & y(N-1) \\ \vdots & \ddots & \vdots \\ y(M-1) & \cdots & y(M+N-2) \end{bmatrix}, \quad \mathbf{a} = \begin{bmatrix} a_0 \\ \vdots \\ a_{N-1} \end{bmatrix},$$

$$\mathbf{b} = \begin{bmatrix} -y(N) \\ \vdots \\ -y(M+N-1) \end{bmatrix} \tag{A7}$$

we assumed that $a_L = 1$ and $M \geqslant N$.

Now, x_i, $i = 1, 2, \ldots, N$, can be easily calculated from equation (A3) and σ_i and ω_i also can be determined. Further details are discussed in references [6, 7].